

The efficiency of thermosyphon solar water heating system and traditional solar water heating system

Ridwan^a, Mahendra Motilal Dhongadi^b, Suheer S Sajjan^c, Imran Mokashi^d

^a Department of Mechanical Engineering, Bearys Institute of Technology Mangalore, India, ridhwan7669@gmail.com

^b Department of Mechanical Engineering, Bearys Institute of Technology, Mangalore, India, mmdhongadi@yahoo.com

^c Department of Mechanical Engineering, Bearys Institute of Technology, Mangalore, India, Sudheersajjan1989@gmail.com

^d Department of Mechanical Engineering, Bearys Institute of Technology, Mangalore, India, mokashiimran@yahoo.com

Article History: Received: 10 January 2021; Revised: 12 February 2021; Accepted: 27 March 2021; Published online: 28 April 2021

Abstract: Loop thermosyphon (LT) is typically used for solar water heaters (SHW) to solve the freezing and corrosion issues. The LT – SWH system has a less night time heat loss compared to conventional SWH due to its thermal diode property but a greater heat loss due to the secondary heat exchange. However, the above interactions have rarely had an effect on system performance based on long-term operation [6]. In this paper, the annual results of above two processes, including productive supply day numbers and efficient heat gains and night power losses, was evaluated in this analysis in two separate operating modes on the basis of standard meteorological year data from the City of Fuzhou. Variations of the above variables are addressed with the change in the stated temperature. The results show that the effective delivery days of the LT – SWH system are 139 and 153, respectively, in irregular heating method. The number of days is 168 to 173 in ongoing heating method.

The SWH system is predictable to have a higher ratio at nighttime with an annual average of 15.07%, which equates to 6.15% for the LT – SWH system. In fact the LT – SWH method results in a lesser decrease in temperature at night and therefore a smaller raise in the temperature on the following day because of multiple relative heat loss factors running at various hours. The results produced are unpredictable, and lead to an approximately successful heat gain for the same month between November and April. The fixed temperature influences substantially the relative quantities of effective annual supply days and effective annual heat gain, slowly reducing the overall dominance of the LT – SWH method and even changing it as the set temperature increases [12]. This shift is triggered by the biggest daily heat loss leading the domination. In combination with a long static reimbursement time, a conventional SWH system must be substituted by an LT - SWH system, particularly when water temperatures are high on demand.

Keywords: Thermosyphon, LT-SWH, City of Fuzhou, Reimbursement, Daytime, NightTime

1. Introduction

In alleviating the electricity shortage, green energies play a significant part. In January 2019, China declared energy output and use of China in the 2018 International Energy Agency (IEA) and National Energy Administration (NEA). It demonstrates the competition of traditional fossil fuels for renewable energies, in particular solar and wind. China is the world's largest producer of renewable energy. A many use case designs in solar energy are widely used for solar hot water (SWH), particularly in the fields of building and in manufacturing. SWH is expected to save about ~kWh of electricity per year [8] with 2 m² collectors.

For a SWH device, the consumers may primarily receive hot water on demand by two heating patterns. Those are constant mode of heating and secondary mode of heating. In the former, the consumer will not drink water when their average temperature does not exceed the defined value; for the following day or days, the mesothermal water is constantly heated up to the set value. This method cannot ensure a daily request for hot water & a significant loss of heat at night. In the case of an anomaly, a subsidiary heater is used for Latin systems to guarantee the need for the everyday hot water. The above form of heating guarantees ideally no heat loss at night, hence heat recovery is the most effective. In the case of aluminum alloy it has good thermal conductivity and good corrosion resistance [16] In this study, in contrast to the constant form, the second heating design is known as the irregular heating method.

Erosion and frost heating are glitches with the traditional SWH method. In fact, opposite flow is usually occurring overnight in SWH thermosyphon systems [10]. This causes significant night heat losers and reduces effective energy production (over 24 hours). This results in significant reverse flows during the night. Three SWH thermosyphon systems were investigated in the night experimental with the total heat loss in **Michaelide et al . (2011)**. During the afternoon the total energy deficit was 40% of the energy obtained during the day [2], according to the findings. Zhang et al. (2017a), an annual performance percentage was calculated and analyzed for the SWH system. The annual normal heat loss was found to be 18 percent of the heat received at nights for the traditional method, and in particular the highest monthly regular heat loss was over 50 percent. In order to quantify the night time heat loss of a SWH unit and to anticipate that any attempt to improve system flow inverted leads to further heat losses in the surrounding environment, which leads to a decrease in overall system heat output, solar link

pipes and storage tanks have also been developed [5]. **Tang et al . (2010)** It is very obvious that the absence of nighttime heat is the increasing energy deficit in a constant heating cycle in a conventional SWH system.

Loop Thermosyphon (LT) is the new methodology for the management of typical SWH system problems. The thermosyphon should be paired with the LT-SWH device in order to prevent freezing and corrosion issues. The loop thermosyphon thermal property prevents reverse water flow into the solar collector from the tank, which is useful to limit thermal losses by night. Fig 1.1. Can contain schematic diagrams. LT-SWH and SWH process norm 1. As shown in the photo. 1, it is easy to replace the common water tank by the bucket water tank to reconstruct an LT – SWH system using a SWH system. According to the previous research of the **writer (Zhang et al., 2016)**, Efficiency can be achieved by not less than a predictable LT-SWH device. The above advantages demonstrate the purpose of the LT-SWH device for hot household water substitute [9]. Nonetheless, fig. However. The second coefficient of the secondary heat exchange device LT-SWH 1 is also found to have decreased heat loss in the afternoon. In this case, the cyclical water temperature is comparatively high, which in continuous heating mode exacerbates this downside. The above-mentioned limitations will obviously impede an LT-SWH device's everyday performance.

In accordance with the best understanding of the author, the method LT-SWH and conventional SWH is primarily under high solar energy or short term activity. The long-term operation seldom relies on the big heat loss factors (the LT - SWH method at daytime, the SWH at night). In the current analysis, the annual efficiency of the two systems in continuous heating modes is analyzed comparatively on the basis of the standard weather year data of the city of Fuzhou. A rise can be seen and addressed in the effective supply days, functional thermal rise and heat loss at night. The relative sizes of these three variables are often influenced by the fixed temperature.

2. Mathematical Model

2.1 Performance Time Evaluation

The photo thermal output of a solar thermo device, β_t , can be measured according to the following (Huang and Du, 1991):

$$\eta_t = \alpha - U \frac{T_i - T_a}{H_t}$$

For T_a , the average daily ambient temperature shall be ° C; H_t shall be ° C as the total ULT radiation; the initial temperature of T_i shall be MJ / m²; α shall be the usual thermal photo output if the initial waters are equal to average ambient daily temperature; U shall be the dawn rate of the temperature loss. In a linear system based on experimental results, α and U values are to be produced. The resulting regression equation can be used to approximate the thermal output of the system in altered climates [11]. The solar collector is usually mounted with a tilt. Yet, yet the solar radiation used in standard environment annual statistics corresponds to the horizontal plane model.

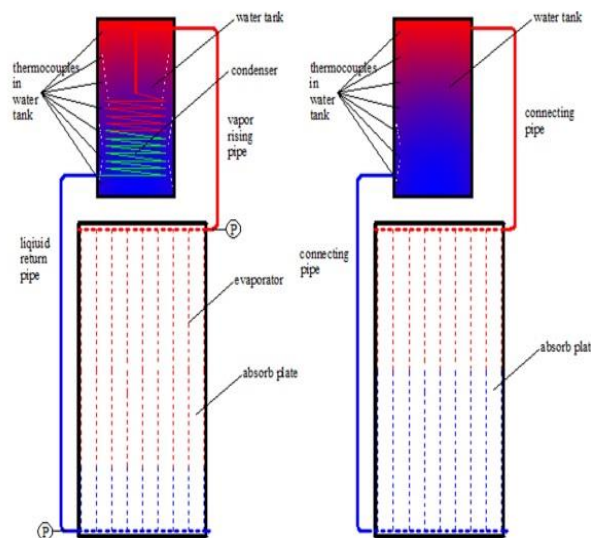


FIG No.1: LT - SWH SYSTEM AS CONVENTIONAL SWH SYSTEMS

The solar energy on the HT- inclined apparent must therefore be measured and expressed as following the horizontal surface results: (Guiana et al., 2001) :

$$H_t = R_b (H_c - H_{cd}) + H_{cd} \frac{1 + \cos(\beta)}{2} + H_{cp} \frac{1 + \cos(\beta)}{2}$$

$$R_b = \frac{\frac{\pi}{180} \omega'_s \sin(\phi + \beta) + \cos(\phi - \beta) \cos(\gamma) \sin(\omega')}{\frac{\pi}{180} \omega_s \sin(\phi) + \cos(\phi) \cos(\delta) \sin(\omega_s)}$$

$$\omega'_s = \min [\cos^{-1}(-\tan(\phi) \tan(\delta)), \frac{\pi}{2}]$$

$$\omega'_s = \cos^{-1}(-\tan(\phi) \tan(\delta))$$

$$\delta = 23.45 \sin\left(\frac{360(284 + n)}{365}\right)$$

Where the H_c is the horizontal radiation W / m², H_{cd} is the horizontal plane distribution, W / m² is the clear layer, usually 0.2; the R_b is a percentage radiation on both a sloping surface and the horizontal plane respectively; the β indicates the vertical latitude; the β is a decrease in the solar angle. They can refer to their performance which are:

$$\text{SWH SYSTEM } \eta_{n,SWH} = 0.547 - 0.052 \frac{T_i - T_a}{H_T}$$

$$\text{LT - SWH SYSTEM } \eta_{nt,SWH} = 0.550 - 0.140 \frac{T_i - T_a}{H_T}$$

Using the calculation above, we can assume again, because of a secondary heat exchange, that the LT – SWH device has a higher heat loss amount.

2.2 : Night - Time Heat Loss Evaluation

If the final water temperature is small at the end of the day or when the initial heating temperature is weak, the fixed value does not fulfill the highest probability of occurring in a continuous heating cycle. Therefore, the original water temperature of the following day will be taken into consideration of nighttime heat loss. However, while a variety of studies include the reverse flow to the solar thermosyphon method, the writers have better information that nighttime heat loss does not have a semi-empirical connection.

Tang et al. (2010), on their studies acquired the primary coefficients for the control equations. Our analyses cannot, however, move directly to the current study. Rather, the coefficients of nighttime heat loss are determined on the basis of the semi-empirical associations reported in this article [15].

The heat loss from the collector surface to the celestial dome is marginal in the solar collector at gloomy times, and heat loss (in units) from the collector to the atmosphere can be represented by

$$mC_p \Delta T = A_c U_l (T_p - T_a)$$

Where m is a collection water mass, the a_c is the collection solar panel of area m², U_l is a coefficient solar panel, W/(m²•k), and T_p represents an absorbent plate's surface temperature, the incapacity to heat is primarily associated with the solar collector at top, back and bottom. The heat loss factor on the roof is calculated properly.

$$U = \left\{ \frac{N}{\frac{c}{T_p} \left[\frac{T_p - T_a}{N + f} \right]^e + \frac{1}{h_w}} \right\} + \frac{\sigma (T_p + T_a) (T_p^2 + T_a^2)}{(\varepsilon_p + 0.00591 N h_w)^{-1} + \frac{2N}{\varepsilon_c} - N}$$

$$f = (1 + 0.0892 h_w - 0.1166 h_w \varepsilon_p) (1 + 0.07866 N)$$

$$c = 520 (1 - 0.000051 \beta^2)$$

$$e = 0.43 \left(1 - \frac{100}{T_p}\right)$$

$$h_w = 5.7 + 3.8V$$

Where N means the glass covers sum and usually the $N=1$; the absorbent layer emissivity c is the surface emissivity of the glass surface; T_p is assumed to be the maximum water temperature at the beginning and end of

the water tank at the appropriate time [12]. A measure of the solar collector's coefficient of heat loss is the thermal resistance of the insulation and thermal convection strength between the solar array and the environment.

$$U_b = \frac{1}{h_w + L_b/\lambda_b}$$

Where the thickness of surgical insulation is L_b , m; λ_b to conductivity of thermal isolation membranes, W/(m•K). The thermal failure rate of the solar collector sheet can be determined by about:

$$U_e = \left(\frac{\lambda_e}{L_e} \right) \left(\frac{A_e}{A_c} \right)$$

Where the thickness of surgical insulation is L_b , m; λ_b to conductivity of thermal isolation membranes, W/(m•K). The thermal failure rate of the solar collector sheet can be determined by about:

The total heat loss measurement of solar collector is therefore as:

$$U_l = U_t + U_b + U_e$$

The situation differs however during clear night, because the shield used for thermal radiation used in collectors for a long wave of radiation is not completely visible (Cook 1985). The absorber's thermal radiation releases through the glass cover and dissipates to the sky dome. Therefore in this scenario, solar collector heat loss can be shown:

$$mC_p\Delta T = A_c U_l (T_p - T_a) - A_c \mu [\epsilon_p \sigma (T_p + 273.15)^4 - Q_{sky}]$$

Where μ is a glass cover, T_a is an atmospheric temperature in real time, °C; Q_{sky} is a function of the celestial dome thermal radiation, J / m². Q_{sky} 's principle of equations will be used to calculate the frequency of heaven's dome thermal radiation by noon [11]. However, the long-wave radiation details are also not important. Therefore, Q_{sky} is calculated as next instead.

$$Q_{sky} = \sigma T_{sky}^4$$

Two heat conductivity resistor components of the insulation content are defined for the connected pipes and the convective thermal resistance between the pipes and the atmosphere:

$$U_p = \frac{1}{h_w + \frac{D_i}{2\lambda_p}}$$

T was studied on the Fan and Furbo (2012a) water tank. Joseph and others. Solar power 197 (2020) 433-442 435 is the temperature-based heat-loss coefficient in various parts of the water tank. The thermal loss limit is as follows:

$$U_w = 2.4 + 0.00198\Delta T$$

The tank should be recharged the next morning if the hot water is spread by night. Nevertheless, in the meteorological year report [8], metropolitan water temperature figures have not been included. If not, the water temperature of the nearby river is used. In order to measure the temperature of the river have identified a correlation between the weather factors. The effects of ambient, humidity and wind speed have been completely considered within the semi-empirical correlation as follows [9].

$$T_i = 4.717e^{0.041T_a}$$

3. Simulation Settings And Overnight Testing Power Failure

3.1 Simulation Setting

The water and solar tank sizes (Zhang et al. 2016; Fan & Furbo, 2012a), which are of the same scale, are compared to 150 liters and 2 m². This refers specifically to a traditional Chinese family of three or four individuals according to Chinese tradition (Wang and Wang, 2008). The mean water temperature is 48 °C (GB / T 19141-2003) as added. While estimating the heat lost at night, Table 1 displays the values of the SWH device and the LT – SWH system parameters.

1. The hot water is only provided at night if the temperature meets the fixed amount and is used up every night. The hot water is therefore consumed during a limited amount of time and thus the lack of power is minimal at that process [12].

2. The temperature decline in the night is also halted at dawn time on the next day. Ice is refilled. This is when solar radiation exceeds zero. The load time is not taken into consideration.

3. The full-day photo thermal output is constant (7) and (8), and it is difficult to estimate even the final water temperature. The final water temperature can under such conditions be higher than the given value; the real final temperatures, and not the set, are often dependent on the effective heat gain.

4. Nighttime temperature drops are minimal. The water temperature cannot be less than 0 ° C and not also under the air temperature.

A program C plus+ recalculates the maximum regular air temperature, gathers meteorological data, assess the photothermal effectiveness of the day and the thermal failure of the night. The annual heating flow map is shown in the diagram. 3.1. As in discontinuous heating the flow diagram is very it does not occur here.

You will see the nighttime simulation effects. The output of the temperature is compatible with experimental results, both systems have medium deviations below 1.5 percent. At the same moment, the rises and falls in the water temperature can be easily shown in the diagram in the left bottom corner in which it is seen that reverse flows exist in the water tank. The internal flow inside the water tank is mainly calculated with the LT – SWH system. The consequence of a fairly high height between the water tank and the collector should also be noted for the SWH device as well as the heat loss by connecting tubing [12].

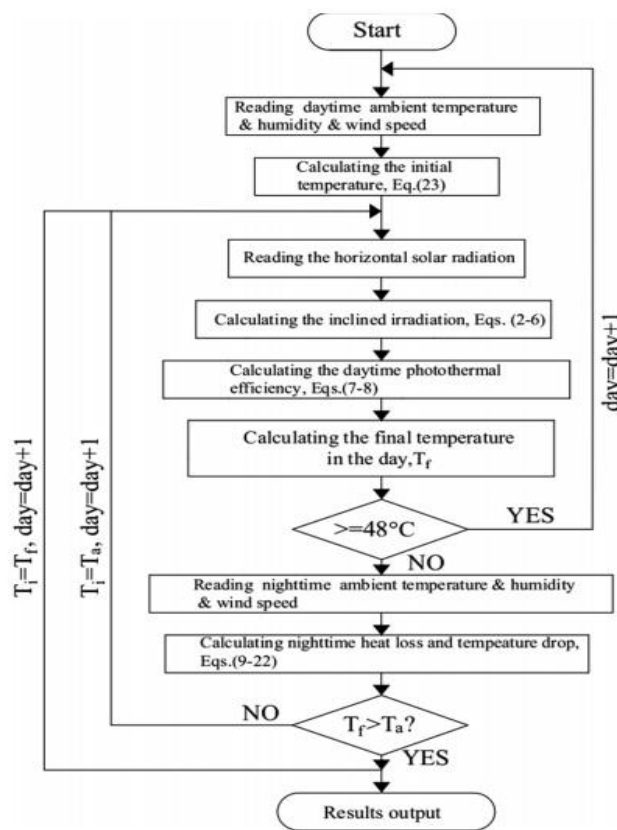


Fig No.3.1: FLOW CHART OF CALCULATION OF ANNUAL PERFORMANCE SYSTEM

3.2 Night Time Heat Loss Validation

Eqs, as previously stated. In (7) and (8) real outdoor experiments were created. All systems may only be tested for productivity during the night. Data have been obtained from earlier studies for the authors of the LT-SWH method and in Zhang et al (2016) the experimental design is extensively available. He and al. (2011) the data for the SWH system at night shall be included. In the meantime, the experimental design of all variables changed during the simulation. The figure shows the results. Description of 3. Description of 3.

4. Result And Discussion

The Fuzhou City (26.08 ° N, 119.30 ° E), China's provincial city, belongs to a subtropical region with a dry monsoon season. Photo. Photo. Image. 4 displays the average monthly external radiation, the average monthly sunshine measurement of the horizontal plane and the inclined plane, and the average monthly climate of the town

of Fuzhou. This is listed below. The calculated monthly R_b indicates a decrease in months and first; the figures vary from 0.85 to 1.85 and in December and June lead to the highest and lowest levels. It's because the solar decline angle; the period angle of sunrise and sunset on the inclined plane THER 's and the horizontal plane there are calculated by R_b . The size of K_{in} 's and K_{in} varies however with the angle of solar decline – and geographical latitude. If $0 > < 23^\circ 24''$, the TRA is equal to $\mu/2$, while the TRAS is increased as the TRAS increases, RB gradually decreases as the μ is increased in the spring equinox to the summer solstice.

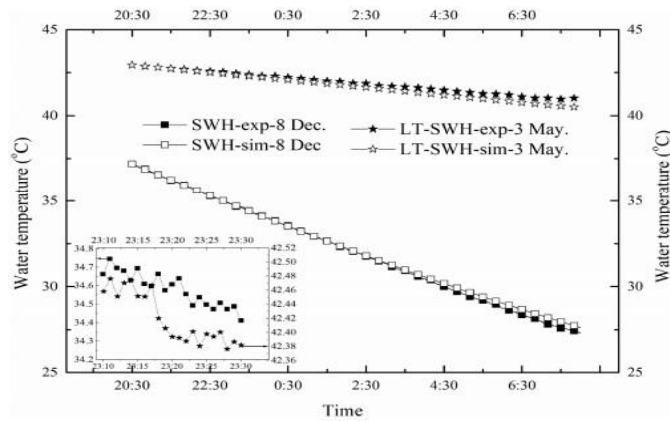


FIG No. 4.1 : SWH PROGRAM OR LT – SWH PROGRAM VALIDATION OF THE NIGHT TIME POWER LOSSES.

When the equinox of the autumnal equinox to the winter surface, $-23^\circ 24''$ is equal to the amount of \pm , the equinox of the autumnal -10° is comparable to a decrease of the $-23^\circ 24''$'s; Although R_b gradually decreases with an increase of μ during the winter solstice to the spring equinox.

The average monthly ambient temperature which first and then decreases, shows an overall trend of increases, varies from 11.9oC to 30.2oC; the minimum and maximum values respectively correspond to January and July. It is noticeable from Eq for the reflection of solar radiation on the inclined floor. (2) if the inclination angle of the collector β is constant, R_b depends linearly on the ratio of direct radiation. Its scale is therefore determined directly by R_b . Therefore the cumular solar radiation on the inclined plane is greater than on the horizontal plane during May to August; while the other months are different. Throughout May to August R_b is less than 1 calculating the range between 266.6 MJ / m², 513.4 MJ / m², for monthly cumulative solar radiation on the inclined surface, and July and February for maximum and minimum levels.

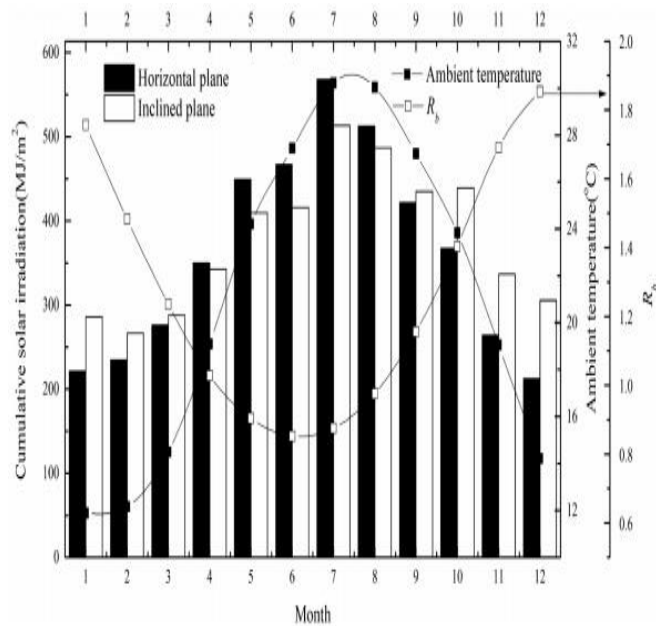


FIG No. 4.2 : VARIATION IN MONTHLY EVERAGE AMBIENT TEMPRATURE

Yearly solar cumulation Only if solar energy is used will the measurement display the monthly effective amounts of supply days in various heating modes of SWH and LT — SWH systems. 5. Efficient supply days shall be defined as the day on which the water temperature exceeds the fixed value[13].

4.1 Effective Days Or Wither Effective Card For Days Even De Effective

Indicates that the effective amount of LT – SWH device supply days shall always be no less than that of the SWH device in keeping with the same month except for June in a continuous heat mode. This is the fault of the LTSWH system's fairly low photo thermal performance. The performance of the interruptible heating mode is less than the continuous heating mode for the same system. It is clear that the efficient amount of supply days of continuous heating is decreased by heat absorption and this impact becomes apparent when the temperature at the same time becomes small even with a low degree of solar radiation.

Moreover, it can be observed fig 5 since, regardless of hardware and heating processes, the mean values for the effective amount of delivery day shall be taken in July. In a stop heating device and continuous heating mode during February, minimum values will be taken in a different month during January. The annual efficacy of the SWH system was measured at 139 and 168 in discontinuous and continuous heating modes, and the annual effective amount of supplies for the LTSWH rose to 153 and 173.

The high initial water temperature and high solar radiation in the summer are also understandable as the efficient supply volumes are associated with the same months but with certain types of heating.

The effective heat gains are shown in the Fig under different heating modes. Comprehensive 6. It indicates that firstly, the successful heat gain in the discontinuous heating mode, which differs from the actual number of supply-days, correlates to the same month. This is mainly that there is no power loss at night, according to the theory. First, in July and February respectively, the average and minimal heat losses are observed.

Second, Fig. Fourth. 6 indicates that the efficient heat gain in the discontinuous heating mode of the SWH method is usually less than that in the same month of the LT – SWH device. In addition, it is because the photo thermal efficiency of LTSWH is greater during the day under these circumstances [14].

The SWH system's effective power gain in continuous heating would therefore be roughly between November and April to that in the same month for the LT-SWH device. However, the relative magnitudes of heat output success between the SWH and the LT-SWH systems adopt the same trend of discontinuous ventilation for the other months. The reasons why the temperature in the water and the loss of heat at night are unpredictable are analyzed thoroughly.

4.2 Comparison Of The Nigh - Ttime Heat Loss

As previously stated, the heat loss at night contributes in the continuous heating mode to less efficient power gains. Similar figures for the monthly overall heat loss by different heating methods are seen in the figure as well as the average monthly night temperature decreases. Details of 7.

Secondly, the heat loss and the decrease of the SWH system's temperature during the night are clearly larger than the SWH system's overnight temperature loss equivalent to the same month. The maximum values of 93,4MJ and 39,7MJ are both taken in February, and the minimum values of 17,1MJ and 5,6 MJ respectively are taken in July. Furthermore, from November to April all devices had larger accumulated power loss. Since, along with Fig. After. 5 The effective number of days in these months is limited due to comparatively low sun exposure and low ambient tempers; comparatively low nighttime ambient temperature, in comparison, leads to higher heat loss coefficients and a higher nighttime loss total. However, hot solar radiation and a high initial water temperature from May to October and in July and August in particular means that the water temperature reaches a value set at the end of the day in most days, which considerably reduces heat losses during the night [15].

Figure shows the heat loss ratios defined as the heat loss per night in the day's heat collection. 8. The trends in the curve can be seen as similar to Fig. 7. Nonetheless, as the overnight heat loss explicitly influences the water temperature of the first day and thus affects the day's performance, the ratios vary considerably. Furthermore, the ratio of night time heat waste to full heat collection (in discontinuous heating mode, according to the heat selection) is always provided as a reference, even though they are not right.

The SWH System calculates a maximum and minimum heat loss ratio of 54.43% and of 3.09%. The values are 22.52 for the LTSWH system and 0.96%, respectively. The SWH program therefore reports an overall annual heat loss ratio of 15.07% while the SWH method's estimated heat loss ratio is 6.15%. For SWH, the maximum heat insufficiency ratio is 12.43 percent, equivalent to the overall heat range, for the LT-SWH it 5.00 series. Seven Fig. Seven and Fig. Picture. 8. We can also infer that the night time losses in the SWH system in continuous heating mode are at least two times greater than those for the LT — SWH device; the effective heat gain therefore differs at least 13 percent. The Fig, however, shows. 6 In the same month roughly from November to April, the real heat rises for such systems are seen, with a 4% difference [12]. The LT-SWH device and SWH operate at various times and are responsible for high heat loss coefficients. Original and final waters for chosen days are seen in January (above) and July (down) to validate the deduction.

For the current five days, the water temperatures are chosen for January. With the photo. The photo. 9, of course, the original water temperature of the LT SWH system is higher on the same day than that of the SWH method, but the final water temperature of the two systems is almost identical. Firstly, the heat loss of LT-SWH, the dominant thermal loss overall, is negligible because of the thermal diode property of the loop thermo syphon. Therefore, during a dissipation night the initial water temperature of the LT – SWH device is higher. The first and second points respond sensitively to this sequence. The higher initial water temperature, however, still operates on the LTSWH system's hot-day failure, contributing to a less powerful photo thermal and hence a smaller increase in temperature. That is, the heat energy allocated to the loop thermosyphon during the night is effectively dissipated during the day under the continuous heating system. The final temperatures thus refer to all structures roughly. A common cycle of cycling often happens between November and April, and this is why the two systems have average values for successful heat gains during certain months.

In July, there are also important indicators that the two systems operate at various periods with large heat loss coefficients. As, in the lower part of the first water temperature of both systems, the final water temperature of the LT-SWH system is the same in the last 3 days, due to a relatively lower photo thermal output. But for the first two points they share with January the same cyclical pattern. The distinction between May and October is that the effective power inputs of the LT- SWH system overweight those of the SWH system in that month, because of the significant amount of productive supply days in both months.

4.3 Comparing The Photo Thermal Efficiency

Figure indicates SWH and LT-SWH in various heating modes average monthly photothermal efficacy. Hold. The first thing that it reveals is the monthly photothermal efficiency of the LT-SWH system in discontinuous heating mode for the same month. Secondly, all devices have a maximal output of equivalent photothermal efficiencies, which tend to be quite counterintuitive. Generally, the municipal waters of China have the characteristic of warm in winter and cool in summer, when compared to the ambient temperature (Zhan, 2017), which means that the expected photo-thermal performance is usually greater than the traditional photo-thermal performance in summer but smaller than the usual photo-thermal performance in winter. Nevertheless, the water temperature of the nearby river used in this analysis is typically less than the urban water and the normal air temperature. The contra intuitive experience is liable for it. Eventually, photo thermal efficacy of the device LT – SWH and the device SWH both display a tendency to rise first and to decrease, although photo thermal efficiencies are approximately equivalent to the comparable system SWH from November to April, close to the pattern of successful heat recovery.

By calculation, the annual photo thermal efficiency of the System is 46.62% in the continuous heating mode whereas it is 48.37% for the LT – SWH system, and 56.52% and 59.53% for the discontinuous heating mode.

4.4 Static Payback Period

The continuous payback times of the two devices were examined in the present analysis in conjunction with the traditional electric water heater and gas water heater. Electricity and natural gas prices are based on the second level of public price, announced by the Power grid of Fujian Province and the Fuzhou Commission for Development and Reform. Prices are RMB/(kWh) of 0.5483 and RMB / m³ of 4.16. The natural gas calorific value is 34 MJ / m³ in China. And the gas water heater's thermal efficiency is 0.88, while the electric heater's thermal efficiency is 0.9 (Yunpin et al. 2012). Relation is made to successful heat gains at a fixed temperature of 48°C. The SWH program and LT – SWH device have initial investments of approx. RMB 2300 and RMB 2900, respectively. SWH expenses include storage (RMB 1000), solar piping network (RMB-800), pipelines and building costs (RMB-500). The collector (RMB-1000), solar pipeline (RMB-1200), ventilation (RMB-100), pipelines and costs of development (RMB-600). The SWH network is contrasted to the SWH Process. The results are given in Table 2.

Table 2. Shows the relatively short statistic payback period in contrast with the electric water heater for the SWH device and the LT – SWH method. This is because natural gas prices per MJ of energy are almost 80 % higher than electricity prices. In comparison, the SWH device provides a longer duration of permanent payback in the same heating process, relative to the SWH method, but the gap is only one year. In total, the static payback period for the SWH system range things from 2.7 to 3,9 years; for the LT-SWH, 3,2 to 4,8 years. Nonetheless, since the LT – SWH device is free of corrosion and frosting issues during warming, the time difference between the two systems is appropriate. LT-SWH is a positive alternative for the conservation of building energy.

Heating Mode		Annual Heat Gain (AHG)	Electric Water Heater (EWH)	Gas Water Heater (GWH)
Discontinuous	SWH	5115.03	2.7	3.2
	LT - SWH	5388.40	3.2	3.9
Continuous	SWH	4219.32	3.2	3.9
	LT - SWH	4378.33	3.9	4.8

TABLE NO 1. THE STATIC PAYBACK PERIODS OF SWH AND LT – SWH SYSTEM

5. Conclusion

The LT-SWH system has a higher heat loss ratio in everyday life than the SWH system, but a smaller heat loss coffee in the night time. On the basis of long term operation the above encounters are rarely reported. The efficiency of the SWH and the LT – SWH method is comparatively evaluated using standard weather year details from Fuzhou Town, in continuous and non-continuous heating modes. Effective heat gain increases and effective delivery times are measured based on the estimated photo thermal efficiency of both systems. The primary results are as follows:

1. The average effective number of days for the distribution of the SWH method for discontinuous and constant heating modes is 139 and 168, whereas the LT-SWH device is between 153 and 173.
2. SWH's heat gain in discontinuous heating mode is always lower than LT-SWH in the same month. However, between November and April the monthly effective heat gains of SWH are similar to those of the LT-SWH method. That is responsible for the large coefficients of heat loss that function at various times. The average annual heat loss level for the SWH network is 15.07% and LT - SWH6.15% by estimation.
3. Not only does the temperature environment substantially affect the efficient thermal gain but the relative scale of both devices often increases. The successful heat recovery from the LT – SWH starts below that of the SWH unit at the last water temperature of no less than 60 °C.
4. The continuous compensation period of the LT – SWH program is a little lengthier than the SWH method, varying from 3.2 to 4.8 years.

As per the literature review suggested that LT – SWH is free from corrosion and freezing problems, it is on demand as compare to the traditional SWH.

References

1. Gupta GL, Garg HP. Design system in natural circulation solar water heaters. 1968;12:163±82 solar capacity.
2. Ng KS. An improved computer software for solar water heater thermal efficiency. 1976;18:183±91 Solar Electricity.
3. Morrison GL, Braun JE. Thermosyphon solar water heating system modeling and working characteristics. 1985;34:389±405 Solar Energy.
4. Hobson PA, Norton B. A nomogram concept for direct solar thermosyphon water heaters. 1989;43:89±95 Solar Electricity.
5. The Typical Meteorological Year for Nicosia Cyprus is produced in Petrakis M, Kambezides S, Adamopoulos AD, Kassomenos P, Michaelides IM, Kalogirou SA, Roditis G, Chrysis I and Hadjgianni A. 1998, 13:381±8. Green Electricity.
6. Fanney AH, Klein SA. Performance at the National Bureau of Standards of Solar Hot Water Systems for measurements and forecasts. 1983;105:311± 21 Solar Energy Engineering;
7. Braun JE, Fanney AH. Thermosyphon heating system concept and assessment. In: Annual Conference of the American Solar Energy Society, Solar Energy Minneapolis programme, MN. 1983. 1983. 283±8 of the following page.
8. Hellenic National Agency, Population and housing survey 2011. Dwelling apps and facilities.
9. S.A. Operation. Kalogirou, R. Agathokleous, G. Barone, A. Buonomano, C. Forzano, A. Palombo, New thermo-plate solar thermal collectors type development and validation: energy and economic optimisation of hot water production in various climate, renewal. 632 – 634 MN MN

10. HEDNO, The PV panels (net-metering system (GR)) commonly asked questions and responses. (15 December 2018 accessed).
11. F.J.-F.J. Aguilar, S. Aledo, P. V. Quiles, Experimental study in the domestic production of heat pumps in residential photo voltaics, *Appl. The gym. Engineering.* 379e389 (2016).
12. K. Khalaf, Carleton University Ottawa, Ontario 2017, Experimental Characterization and Modeleration of Heat Pump Water Heater.
13. S. The report evaluating the new EU energy-efficiency policy system and presenting policy recommendations on choosing to reach cost-effective power-efficiency / savings capacity through 2020 or beyond, 2014, 2014, at 204. Braungardt, W Eichhammer, R. Elsland, T. Fleiter, M. Klamasa, M. Krail, B. Pfluger, M. Reuter, B. Schlomann, F. Sensfuss, T. Sohaib, Braungardt, W.
14. L. Steinbach, D. Staniaszek, Buildings Performance Institute Europe (BPIE), 2015. Discount rates of the energy system study.
15. Hellenic Statistical Authority, 2011 population and housing census.
16. Sajjan, S. S., Kulkarni, M. V., Ramesh, S., Sharath, P. C., Rajesh, R., & Kumar, V. (2019). Mechanical and Microstructural Properties of Multi-Axially Forged LM6 Aluminium Alloy. In *Advances in Manufacturing Technology* (pp. 131-139). Springer, Singapore.